ELSEVIER

Journal of Organometallic Chemistry 486 (1995) 79–93

Journal of Organometallic Chemistry

Synthetic and theoretical MO calculational studies of lithiotriazine intermediates produced during alkyllithium-induced cyclotrimerisation reactions of organic nitriles, and comparison of their structures with that of a methylmagnesiotriazine derivative

David R. Armstrong [a], Kenneth W. Henderson [a], Murray MacGregor [a], Robert E. Mulvey [a,*], Michael J. Ross [a], William Clegg [b], Paul A. O'Neil [b]

[a] *Department of Pure and Applied Chemistry, University of Strathclyde, Glasgow G1 1XL, UK*
[b] *Department of Chemistry, University of Newcastle, Newcastle upon Tyne NE1 7RU, UK*

Received 30 March 1994

Abstract

Benzonitrile can be readily cyclotrimerised by treatment with a suitable alkyllithium to give a simple triazine or to a solvated lithiodihydrotriazine derivative. Which cyclic product dominates depends mainly on the source of the active Li^+ cation (*n*-butyllithium, *t*-butyllithium and tetramethylguanidinolithium are considered here), and on the solvent employed. X-ray crystallographic studies on a representative compound show that the lithio species exists as a mononuclear, contact ion pair structure, with the triazine ring in a 1,4-dihydro state. On reaction with the Grignard reagent, MeMgCl, this compound gives a methylmagnesiodihydrotriazine, which has also been crystallographically characterised and found to closely resemble its lithio precursor. Ab initio MO calculations on model systems reveal that the 1,4-dihydrotriazine arrangement is energetically preferred to the 1,2-dihydro alternative irrespective of the counterion (Li^+ or H^+) present. A theoretical investigation of the methanolysis of the lithio species indicates that the formation of an intermediate MeOH complex, with the alcohol attached to a ring N atom and not to Li^+, directs the reaction towards ultimate formation of a 1,2-dihydrotriazine.

Keywords: Triazine; Lithium; Magnesium; Ab initio; Crystal structure

1. Introduction

Compounds belonging to the heterocyclic s-triazine family have been known for over two centuries [1]. Depending on the nature of the substituents attached to the symmetrical C_3N_3 ring, such compounds have found extensive use in the polymer, pharmaceutical and dye industries [1], amongst others, with melamine and cyanuric chloride being particularly important industrial commodities. Their synthetic chemistry has grown in parallel with their commercial utility, and established methods of preparation are both numerous and varied. Given their widespread applicability in other areas of synthetic chemistry [2], surprisingly little attention has been paid to the use of organolithium reagents in triazine synthesis, especially as it was reported over fifty years ago that *n*-butyllithium could bring about cyclotrimerisation of benzonitrile to give a dihydrotriazine [3]. A recent review of dihydrotriazines made by this method and others, drew attention to the fact that such species still require proper structural study, by modern instrumental techniques [4]. In a recent communication [5] we revealed that it was possible to obtain such structural information, not only on dihydrotriazines, but also on lithiotriazine intermediates formed during the conversion of benzonitrile to a triazine. Usually this involves the action of *n*-butyllithium followed by hydrolytic work-up, but in our case we isolated active lithiotriazine contact ion pairs existing prior to the hydrolysis step.

This direct strategy is further exploited in the present study. The solvent dependency of this cyclotrimerisation sequence is closely scrutinised as is the effect of employing a different alkyllithium (*t*-butyllithium) and of replacing benzonitrile by trimethylace-

* Corresponding author.

SSDI 0022-328X(94)05030-F

tonitrile. Lithioketimines [6] can be formed as intermediates in these cyclotrimerisation processes or as products, depending on the stoichiometry used, so that the reaction between benzonitrile and tetramethylguanidinolithium (strictly a guanidide rather than a ketimide, though it belongs to the same structural family) is also considered. In addition, a magnesiotriazine complex is reported and its structure determined by an X-ray diffraction study, to our knowledge this is the first such compound to be crystallographically characterised, and the structure is compared with that of its parent lithio complex. In addition to these experimentally-based studies, ab initio MO calculations have been performed to examine the question of why the preferred structure of the dihydrotriazine anion changes from a 1,4-dihydro to a 1,2-dihydro arrangement when the countercation is changed from Li^+ to H^+, and to shed light on the mechanism of this exchange reaction, which was achieved experimentally by methanolysis.

2. Results and discussion

2.1. The influence of the reaction solvent on the butyllithium-induced cyclotrimerisation of benzonitrile

We found the outcome of the reaction between *n*-butyllithium and three molar equivalents of benzonitrile to be markedly solvent dependent. In hexane alone, the alkyllithium appeared simply to catalyse the trimerisation to give the fully-unsaturated, triphenyltriazine **1** in 58% yield (Eq. (1)) and THF could be added at a later stage to aid crystallisation of the product. However, the presence of THF (mixed with hexane) at the onset of the reaction led to addition trimerisation, whereby formally the lithium reagent

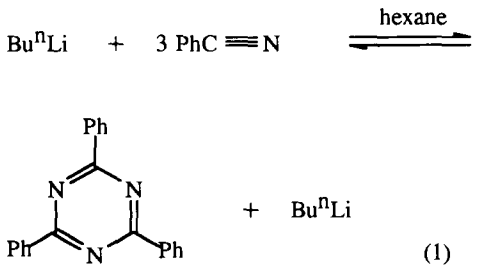

(1)

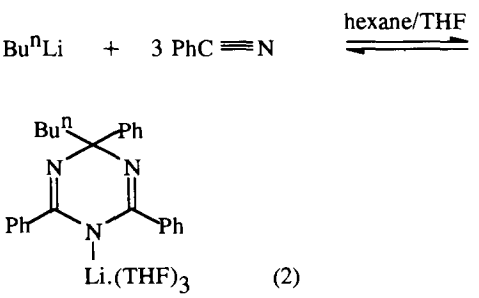

(2)

adds across one of the unsaturated bonds in the six-membered cyclic ring, to afford the lithiodihydrotriazine **2** in 79% yield (Eq. (2)). Significantly, this ring-attached Li^+ centre is tris-solvated by THF molecules. Two previous studies, separated by about forty years, the first by Anker and Cook [3], and the second by Cook and Wakefield [7], employed benzene as the reaction medium and so this solvent effect went undetected. Logic dictates that the formation of **1** is preceded by that of an ephemeral addition species **3**, akin to **2** but unsolvated, which then loses an organolithium compound to leave the neutral triazine species. Either the alkyllithium ^{n}BuLi or the aryllithium PhLi could in theory be eliminated from the triazine ring. In practice, however, only the former compound appears to do so, even though the latter, having the greater ionic character, is the more stable organolithium. Therefore the relative stabilities of the possible triazine products must be the overriding factor in determining the final course of the reaction sequence in this particular case. In this regard, there is a preference for the Ph ring, not the Bu chain, to remain attached to the C_3N_3 ring in order to maximise the resonance contribution to the bonding. The triphenyl-substituted triazine **1** is particularly stable in this respect, as resonance delocalisation is feasible over its entire tetracyclic framework. What prompts the elimination step in the first place? Given that it occurs in THF/hexane mixtures, but not in hexane alone, then the most obvious feature to consider in seeking an answer to this question is the solvation of the metal centre. The availability of the strongly solvating THF prior to the initiation of the cyclotrimerisation process, ensures high coordination (four, on crystal structure evidence (vide infra)) for a C_3N_3 ring-attached Li^+ centre. Adequate stabilisation is thus provided to prevent a subsequent elimination reaction. On the other hand, with hexane unable to function as a Lewis base and with no scope for aggregation due to the steric demands of the substituted C_3N_3 ring, a ring-bound Li^+ centre devoid of THF would be in an excited, low-coordinate state, formally bonding at only one site (N). Such a Li^+ centre, being labile, would encourage the lithiodihydrotriazine structure to release $(^n\text{BuLi})_n$ which, in turn, would aggregate. As well as confirming the hexameric ($n = 6$), distorted-octahedral arrangement long suspected to exist from solution studies, a recent low-temperature X-ray diffraction analysis of butyllithium [8] revealed Li–βC interactions in addition to expected Li–αC ones, making each Li^+ centre four-coordinate overall. Hence the formation of $(^n\text{BuLi})_6$ is coordination based. Introducing THF to the reaction mixture after ^{n}BuLi has been eliminated from the triazine ring (i.e. seemingly too late to stabilise the lithiodihydro intermediate **3**), probably serves only to generate an $[^n\text{BuLi.(THF)}_x]_n$ solution complex, and as it transpires, to facilitate crystallisation of the

triazine **1**, which beforehand existed as an oil. Furthermore, the recovery of **1** also suggests that the addition reaction shown in Eq. (3) is not reversible to any great extent under the mild conditions used (slight warming) and the timescale needed (a few minutes) to effect crystallisation of **1**. However, Wakefield had earlier shown [9] that addition transformations of this type are possible provided the organolithium reagent is in excess and that the reaction mixture (in ether solution) is stirred for a considerably longer period (several hours). On the weight of evidence presented here, we conclude that in this specific system (^{n}BuLi + 3PhC≡N), a coordinating solvent (THF) is necessary to stop the cyclotrimerisation process at the lithiodihydrotriazine intermediate stage, whereas a non-coordinating solvent (hexane) pushes the process further along, to yield a triazine and an organolithium aggregate.

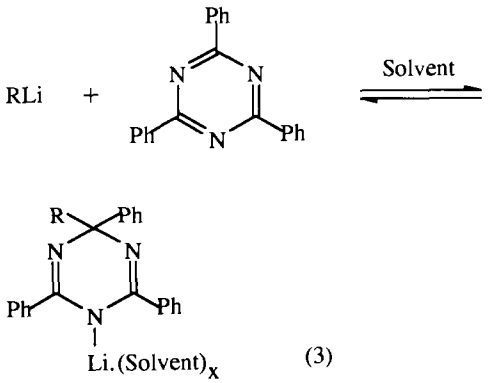

(3)

It must be emphasised that we arrived at the above conclusion on the basis of solid products identified. This approach meant that these solids were isolated directly from active lithium-containing solutions. Cook and Wakefield, in contrast, quenched their solutions with ice and then carried out quantitative analyses of the hydrolysed species so obtained [7]. Their findings clearly suggest that 1BuLi:3PhC≡N mixtures do not give "clean" reactions under the conditions studied (Table 1 lists the various products formed and their respective yields). However, each of the non-triazine products can be accounted for by incorrect stoichiometries of reacting species at localised centres within the solutions: the ketone Ph(^{n}Bu)C=O can be attributed to a 1:1 stoichiometry (Eq. 4), while the isomeric enamidines **4** and **5** are tautomers of the di-imide **6**, which can be attributed to a 1:2 stoichiometry (Eq. (5)). Obviously such stoichiometric-sensitive syntheses require a prior accurate standardisation of the organolithium reagent. If the relative molar ratio of ^{n}BuLi to PhC≡N is assumed to be precisely 1:3 in the solution overall and that the solution is adequately stirred, then why should local variations in stoichiometry occur? The fact that a large amount of "unreacted" benzonitrile (36%) was recovered from the reaction mixture may have some bearing on this question. Our proposal that

Table 1
Products from Cook and Wakefields reaction of *n*-butyllithium with benzonitrile (three molar equivalents) in benzene (yield, %)

1-phenylpentan-1-one	(23)
Enamidine **4**	(27)
Enamidine **5**	(7)
Dihydrotriazine **2** [a]	(29)
Triazine **1**	(2)
Benzonitrile (recovered)	(36)

[a] Identified as the dihydrotriazine obtained after hydrolysis of the lithio species **3**.

the participation of a donor solvent is necessary to form the lithiodihydrotriazine in preference to the triazine appears at first glance to contradict the results in Table 1. The amount of dihydrotriazine formed far outweighs the amount of triazine produced (29% as against 2%), yet surprisingly the reaction solvent was non-coordinating benzene. However, this observation would be entirely reasonable if some of the benzonitrile behaved not as reactant molecules but as Lewis base solvent molecules that could coordinate to, and thereby stabilise, the Li^+ cations attached to the dihydrotriazine ring. Significantly the experimental procedure offered the opportunity for such an event as the organolithium reagent was added to the bulk benzonitrile solution, so that excess (greater than three molar equivalents) benzonitrile molecules would be present at all times until the addition of the organolithium was complete. Subsequent hydrolysis to afford the dihydrotriazine and LiOH would at the same time free solvat-

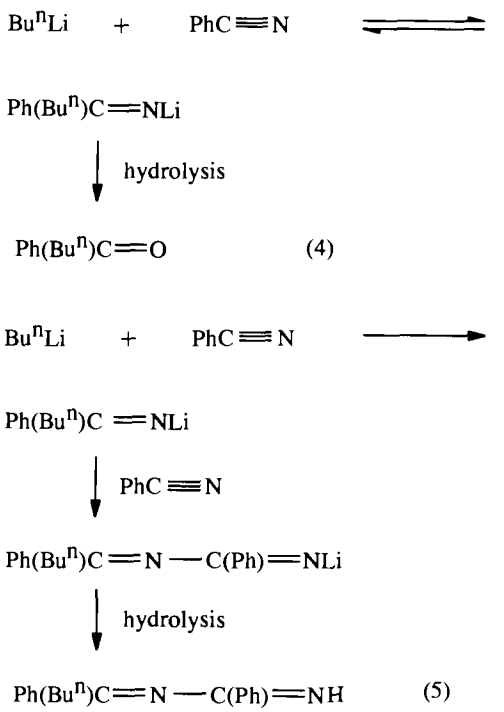

(4)

(5)

ing benzonitrile molecules, and this would account for the fact that so much is recovered from the reaction mixture.

Compelling evidence for the existence of such benzonitrile adducts was obtained when the reaction was repeated with an even greater overall excess of benzonitrile present. The molar ratio of ^{n}BuLi:3PhC≡N used in the earlier experiments was increased to 1:5 (Eq. (6)). Only an oil could be obtained when the reaction was considered in hexane, but addition of THF produced a solution which in turn deposited a yellow solid on cooling. This solid proved not to be the triazine **1**, but the bis(THF)/mono(benzonitrile) adduct of the lithiodihydrotriazine **7**. As yet, we have been unable to grow single crystals of this novel mixed-donor adduct. Characterisation was instead achieved by microanalysis and ^{1}H NMR spectroscopy (unlike **7**, the *t*-butyl isomer **8** proved amenable to mulling in Nujol and so IR spectroscopic evidence was also obtained; the principal feature was the γ(C≡N) band at 2240 cm^{-1}).

$$Bu^{n}Li + 5PhC{\equiv}N \xrightarrow{\text{hexane/THF}}$$

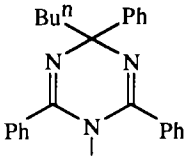

Li.(N≡CPh).(THF)$_2$ (6)

This additional information calls for a qualification to our original conclusion; namely that in order to encourage formation of a dihydrotriazine species, the lithio intermediate must be adequately solvated, whether this be by an externally-added donor solvent (THF) or by unchanged (in the sense that the C≡N triple-bond remains intact) benzonitrile molecules.

2.2. The effect of replacing normal-butyllithium by its tertiary-butyl isomer on the cyclotrimerisation process

More insight into the chemical process preceding the cyclotrimerisation step was gained on examining the action of ^{t}BuLi on PhC≡N. Dropwise addition of PhC≡N to a pentane solution of ^{t}BuLi initially produced a red solution, and then as the stoichiometric ratio approached 1:1 a yellow solid separated. This solid remained undissolved as the addition of PhC≡N was continued until the final molar ratio was 1^{t}BuLi:3PhC≡N. An analysis of the solid revealed it to be the known hexameric lithium ketimide [{Ph(^{t}Bu)C=NLi)$_6$], **9**; one of a family of such compounds, the structures of which have been discussed alongside other N–Li structures in two recent reviews [10]. Its appearance here, coinciding with the 1^{t}BuLi:1PhC≡N stage

$$Bu^{t}Li + 3PhC{\equiv}N \xrightarrow{\text{pentane/THF}}$$

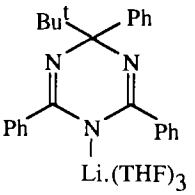

Li.(THF)$_3$ (7)

of the addition sequence, was expected as this was the stoichiometry used to obtain it previously. Since formation of **9** by this nitrile insertion procedure is thought to be near quantitative, and since none visibly appeared to dissolve on charging the mixture with two further molar equivalents of PhC≡N, the implication is that cyclotrimerisation has occurred to a negligible extent, or not at all, at this juncture. Introducing THF to this mixture firstly promotes dissolution of the ketimide **9** and secondly initiates the cyclotrimerisation process. This culminates in a high yield (91%) of the tris (THF) solvated lithiodihydrotriazine **10** (Eq. (7)), in keeping with the rationale that the availability of coordinating molecules, prior to cyclotrimerisation, favours the Li^{+}-(dihydrotriazine^{-}) contact ion pair species over the triphenyl-triazine **1**, as shown earlier for the ^{n}BuLi system. Solvation apart, the formation of **1** is less likely in this case anyway as it requires the regeneration of the highly reactive, tertiary carbanionic ^{t}BuLi. Similarly, the reverse (addition) reactions of the type represented by Eq. (3) would be more favourable for ^{t}BuLi than for ^{n}BuLi on thermodynamic grounds.

As alluded to earlier, another aspect of the ^{t}BuLi system which matches that of the ^{n}BuLi system, is in the formation and solidification of adducts incorporating coordinated benzonitrile molecules. Two THF molecules also bind to the Li^{+} centres of these adducts (**7** and **8**), which are probably structurally analogous to the *n*-butyl/*t*-butyl dihydrotriazine tris (THF) solvate, **11**, whose crystal structure is discussed below.

2.3. The effect of replacing one molecule of benzonitrile by trimethylacetonitrile on the cyclotrimerisation process

Formally introducing a Ph ring in place of a ^{t}Bu group at the saturated C site of the C_3N_3 heteroatomic ring made it possible for us to obtain crystallographic evidence of the make-up of the lithiodihydrotriazine solvates. Experimentally this involved treating a hexane solution of ^{n}BuLi with a molar equivalent of trimethylacetonitrile, ^{t}BuC≡N, to generate in situ the ketimide [{^{n}Bu(^{t}Bu)C=NLi}$_n$], **12**, which characteristically imparts a pale green tinge to the solution. In contrast to

its aryl(alkyl) relation **9**, this compound remains dissolved in hydrocarbon media, even at sub-ambient temperatures. The crystal structure of **9** is hexameric with a central core of two stacked $(LiN)_3$ rings [6]. Such crystallographic characterisation has not yet proved possible for **12** though this compound can be isolated in solid form (albeit in a low yield, reflecting its high solubility), from petroleum ether solutions at −20°C. However, it is reasonable to assume that it adopts the same gross hexameric arrangement as that of **9**. Therefore, its enhanced solubility can be attributed to the presence of the six *n*-butyl chains projecting outwards from the $(LiN)_6$ core. Injecting two molar equivalents of benzonitrile into the solution of **12** initially produced an oil. This behaviour followed the same pattern as the ^{n}BuLi/3PhC≡N/hexane system. But whereas the latter combination gave the triazine **1** on the subsequent addition of THF, the ^{n}Bu(^{t}Bu)C=NLi/2PhC≡N-/hexane system gave the tris (THF) solvate of 1-lithio-4-*n*-butyl-4-*t*-butyl-2,6-diphenyl-1,4-dihydro-*s*-triazine, **11**, in 88% yield (Eq. (8)).

$$Bu^{n}(Bu^{t})C{=}NLi \quad + \quad 2PhC{\equiv}N \xrightarrow{\text{hexane/THF}}$$

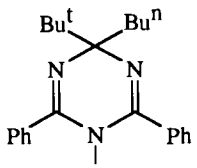

(8)

Had the latter system mimicked the former then the cyclic product would have been a mono(alkylated) triazine (either **13** or isomeric **14**, depending on whether ^{t}BuLi or ^{n}BuLi, respectively, had been eliminated from the C_3N_3 ring), and not the lithiodihydro solvate **11**. The fact that the two systems differ, strongly suggests that the cyclotrimerisations are reversible processes. Lower resonance stabilisation energies for **13** and **14** in comparison to that of the fully-delocalised triazine **1** would shift the equilibrium to the left in Eq. (9). In contrast, the equilibrium would lie to the right in Eq. (1).

$$Bu^{n}(Bu^{t})C{=}NLi \quad + \quad 2PhC{\equiv}N \rightleftharpoons$$

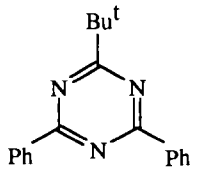

$$+ \quad Bu^{n}Li$$

(9)

Once THF is added to the solution in Eq. (9), the hexameric lithium ketimide is deaggregated to a (presumably) monomeric complex, with enhanced carbanionic nature, which could then attack the benzonitrile to produce a solvent-stabilised, and thus a more-permanent, (lithiodihydro) C_3N_3 ring structure. Some support for this explanation comes from a previous NMR spectroscopic study [11] which unequivocally established that THF does indeed break down the ketimide in question. However, the complex formed is not the expected donor-acceptor species $[\{^{n}Bu(^{t}Bu)C{=}NLi.(THF)_x\}_n]$, but rather the aza-allyl tautomer $[\{CH_3CH_2CH_2C(H)\cdots C(^{t}Bu)\cdots N(H)Li(THF)_x\}_n]$. This transformation involves proton migration from the α-CH_2 unit of the ^{n}Bu chain to the imido N atom. Presumably, the reverse process, intermolecular transfer of the N-attached proton to the α-C atom, is hindered by steric restrictions imposed by the ^{t}Bu group on the adjacent (imido) C atom. The existence of such Lewis base induced aza-allyl species, thought to be general for lithium (or sodium) ketimides with proton-bearing α-C atoms, also implies that the equilibrium shown in Eq. (9) is likely to be inherently more complicated than it is represented. Enamidines (formally di-addition intermediates - vide supra), almost certainly involved, can incidentally be thought of as arising from the direct interaction between benzonitrile and aza–allyl molecules, since the N–H linkage of the latter reactant remains intact in the enamidine product (Eq. (10)).

$$CH_3CH_2CH_2C(H)\cdots C(Bu^{t})\cdots N(H)Li \quad + \quad PhC{\equiv}N$$

$$\Big\Vert \quad \text{hydrolysis}$$

$$CH_3CH_2CH_2C(H){=}C(Bu^{t})—\underline{NH}—C(Ph){=}NH \qquad (10)$$

2.4. The nature of cyclotrimerisation on reaction of tetramethylguanidinolithium with benzonitrile

Tetramethylguanidinolithium $[\{(Me_2N)_2C{=}NLi\}_6]$, **15**, made by lithiation of the commercially available parent guanidine, is a member of the same hexameric structural family as the aforementioned ketimide **9** [6]. In the final cyclotrimerisation system examined by us, a hexane solution of **15** was treated with two molar equivalents of benzonitrile, resulting in the rapid precipitation of a brownish solid. Recrystallisation from a hexane/toluene mixture gave colourless needles, identified by NMR spectroscopy as the mono(dimethylamido)-substituted triazine **16**. Any thoughts that the presence of external donor molecules is intrinsic to the occurrence of the cyclotrimerisation phenomenon can be clearly dismissed by this observation since the solution was donor-free. However, as stated earlier (in Sections 2.1 and 2.2), it must be borne in mind that

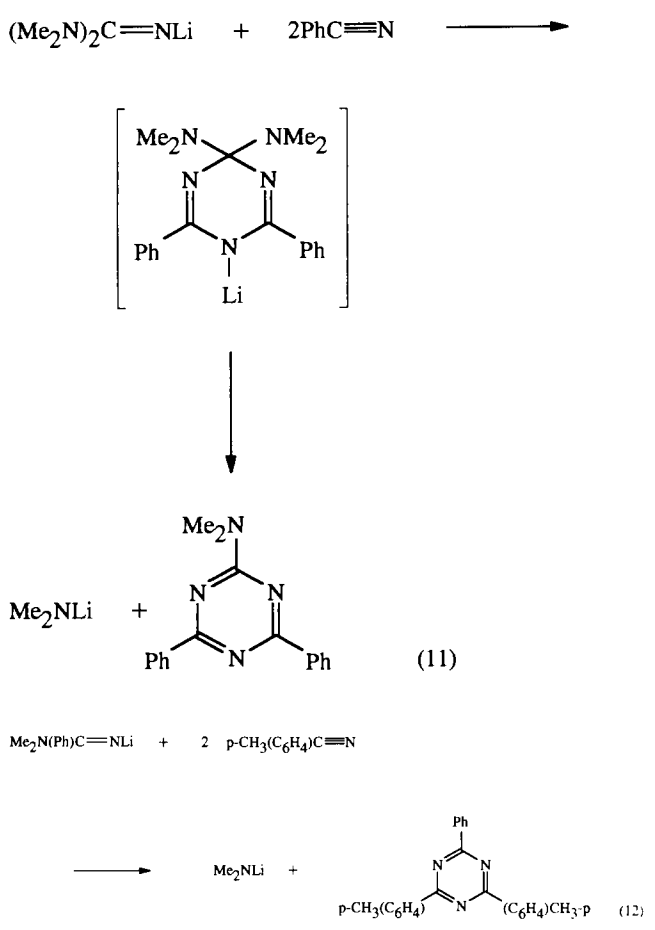

(11)

(12)

benzonitrile can behave both as a reactant, and as a Lewis base towards organolithium compounds. It is therefore a moot point whether any of the RLi/(excess)PhC≡N solutions studied here can truly be described as being donor-free. Significantly, contrary to the three previously discussed systems (in 2.1, 2.2 and 2.3), in which external donor (THF) molecules were available prior to benzonitrile addition, the final product is not a lithiodihydrotriazine solvate (in this case, **17**). Instead, as in the THF-free solution, triazine **16** was obtained in a near-quantitative yield. However, the mechanistic pathway almost certainly involves transient formation of **17**, followed by elimination of the lithium amide $[(Me_2NLi)_n]$ and concomitant production of the neutral triazine **16** (Eq. (11)). The driving force behind this event would be twofold: formation of a stable lithium amide aggregate which increases the number of (anionic) N–Li contacts, and, of course, formation of an aromatic species (**16**). But clearly the former factor dominates since no solvent effect is observed in this system; i.e. even solvent (THF) stabilisation of the C_3N_3 ring attached Li^+ centre cannot prevent $[(Me_2NLi)_n]$ elimination. A virtually identical elimination reaction was reported by Sanger [12], who treated an ethereal solution of the ketimide $[\{Me_2N(Ph)C{=}NLi\}_6]$ with *p*-tolunitrile (two molar equivalents) to give a triaryl-triazine as well as the lithium amide (Eq. (12)).

From this experimental survey we can conclude that the alkyllithium-induced cyclotrimerisation reactions are profoundly sensitive to changes in conditions. The precise stoichiometry, choice of solvent, and the nature of the substituents attached to the C_3N_3 ring, are especially important in determining which product dominates in the competition between lithiodihydrotriazines and triazines. Electron-donating solvents, by

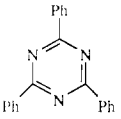

1

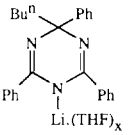

2; x = 3
3; x = 0

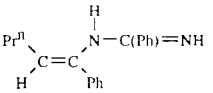

4

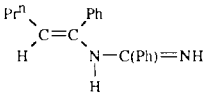

5

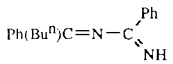

6

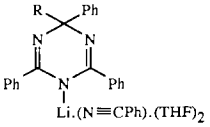

7; R = Bu^n
8; R = Bu^t

$[Ph(Bu^t)C{=}NLi]_6$

9

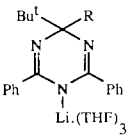

10; R = Ph
11; R = Bu^n

$[Bu^n(Bu^t)C{=}NLi]_n$

12

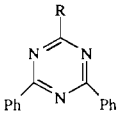

13; R = Bu^n
14; R = Bu^t
16; R = NMe_2

$[(Me_2N)_2C{=}NLi]_6$

15

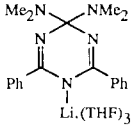

17

satisfying the coordinative demands of the strongly-polarising Li^+ cation in a contact-ion pair structure, can direct the reaction towards the former species. However, the stabilising effect of the coordinating solvent can be overridden by C_3N_3-ring substituents capable of forming highly stable aggregates with the alkali metal. This action favours formation of the latter aromatic species, as illustrated by the amido substituent to lithium amide transformation observed in the final system examined (Eq. (11)).

2.5. Comparison of the structures of a lithiodihydrotriazine solvate and a closely related alkylmagnesio derivative

In a digression from the principal theme of this study, we decided to investigate the chemical reactivity of the newly-discovered, "intermediate" lithiodihydrotriazine species. Thus the solution of a metathesis reaction of the solvate **11** with the Grignard reagent MeMgCl dissolved in THF solution (Eq. (13)) was examined. To ensure better stoichiometric control and to avoid possible side reactions due to the presence of byproducts from the cyclotrimerisation procedure, reactant **11** was preformed, isolated, weighed out in a dry box and redissolved in toluene solution prior to addition of the magnesium reagent. The metathesis proved straightforward, instantly giving a precipitate of LiCl, which was removed by filtration, while the filtrate produced a large crop of the crystalline magnesio solvate **18**. This compound was then subjected to an X-ray diffraction study, to the best of our knowledge it is the first Mg-triazine species to be so characterised.

Inspection of its molecular formula shows that it bears a close resemblance to the lithio solvate **11**. In fact, the only distinction, necessitated by valency considerations, is that one THF ligand of the latter compound has been replaced by a methyl carbanion in the former. Significantly this similarity carries over to their crystal structures (Fig. 1 shows that of **18**; that of **11** has been reported before [5], but for comparison it is shown again in Fig. 2). This situation is unusual, for even isoleptic Li and Mg compounds tend to exhibit pronounced structural differences as is borne out by recent reviews of the crystal structures of organolithium compounds (in 1985) [13] and organomagnesium compounds (in 1991) [14]. Therefore these crystal structures provide a rare, but not unique, example of experimentally-determined data with which to gauge the steric and electronic consequences of substituting "Mg^{2+}" [formally $(MgMe)^+$] for "Li^+" in a chemi-

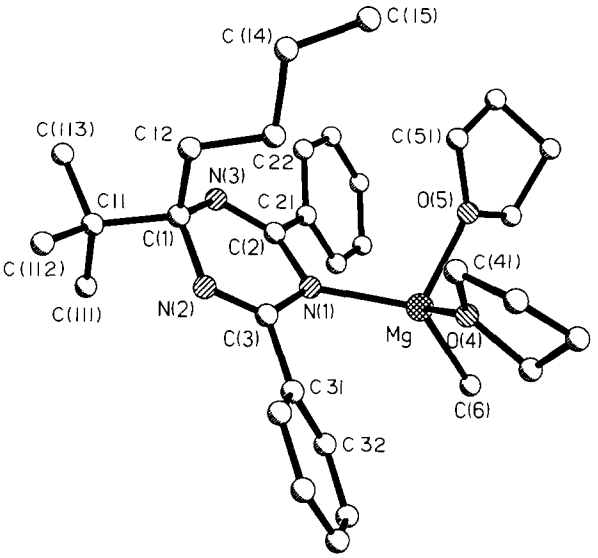

Fig. 1. Molecular structure of the magnesiotriazine **18** with hydrogen atoms omitted.

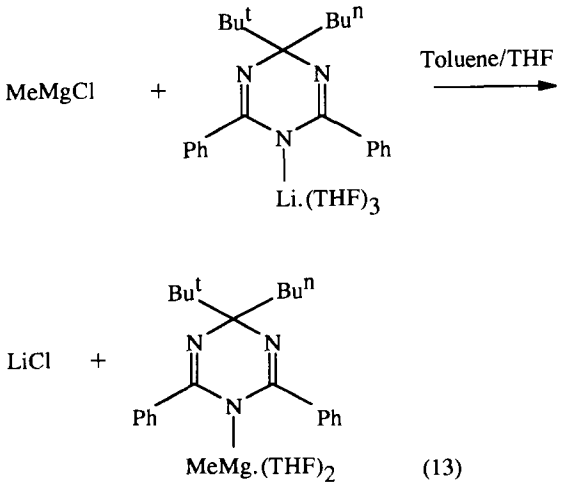

(13)

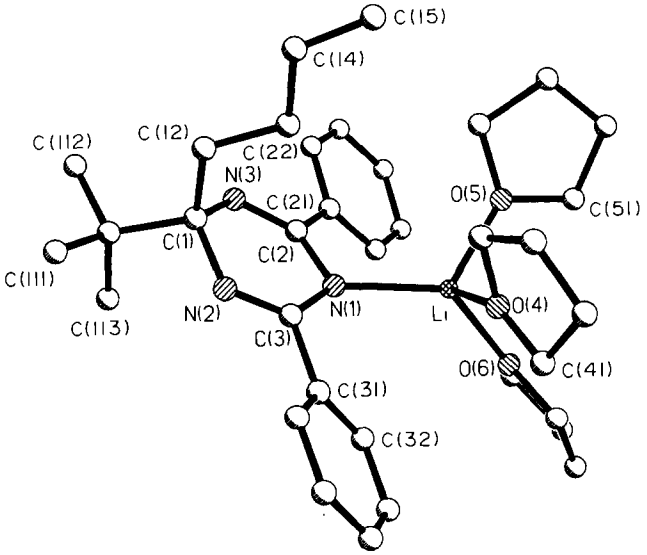

Fig. 2. Molecular structure of the lithiotriazine **11** with hydrogen atoms omitted.

Table 2
Bond lengths (Å) and angles (°) for **11**

N(1)–C(3)	1.371(4)	N(1)–C(2)	1.386(4)
N(1)–Li	2.059(8)	N(2)–C(3)	1.291(4)
N(2)–C(1)	1.475(4)	N(3)–C(2)	1.287(5)
N(3)–C(1)	1.457(5)	Li–O(4)	2.025(10)
Li–O(4A)	2.015(10)	Li–O(5)	1.958(13)
Li–O(5A)	2.035(11)	Li–O(6)	2.091(10)
Li–O(6A)	1.968(11)	O(4)–C(44)	1.419(7)
O(4)–C(41)	1.433(7)	C(41)–C(42)	1.476(9)
C(42)–C(43)	1.382(12)	C(43)–C(44)	1.469(8)
O(4A)–C(44A)	1.420(7)	O(4A)–C(41A)	1.435(7)
C(41A)–C(42A)	1.476(8)	C(42A)–C(43A)	1.379(12)
C(43A)–C(44A)	1.465(8)	O(5)–C(54)	1.421(7)
O(5)–C(51)	1.430(7)	C(51)–C(52)	1.474(8)
C(52)–C(53)	1.374(12)	C(53)–C(54)	1.470(8)
O(5A)–C(54A)	1.423(7)	O(5A)–C(51A)	1.434(7)
C(51A)–C(52A)	1.466(8)	C(52A)–C(53A)	1.386(12)
C(53A)–C(54A)	1.471(8)	O(6)–C(61)	1.415(7)
O(6)–C(64)	1.433(7)	C(61)–C(62)	1.470(8)
C(62)–C(63)	1.385(13)	C(63)–C(64)	1.476(8)
O(6A)–C(64A)	1.415(7)	O(6A)–C(61A)	1.433(7)
C(61A)–C(62A)	1.477(8)	C(62A)–C(63A)	1.395(13)
C(63A)–C(64A)	1.476(8)	C(1)–C(12)	1.532(6)
C(1)–C(11)	1.562(6)	C(11)–C(111)	1.527(8)
C(11)–C(113)	1.528(8)	C(11)–C(112)	1.532(6)
C(12)–C(13)	1.477(7)	C(13)–C(14)	1.515(7)
C(14)–C(15)	1.369(12)	C(2)–C(21)	1.489(5)
C(21)–C(26)	1.385(5)	C(21)–C(22)	1.384(5)
C(22)–C(23)	1.380(6)	C(23)–C(24)	1.370(7)
C(24)–C(25)	1.377(6)	C(25)–C(26)	1.388(6)
C(3)–C(31)	1.496(4)	C(31)–C(36)	1.372(5)
C(31)–C(32)	1.383(5)	C(32)–C(33)	1.384(5)
C(33)–C(34)	1.368(6)	C(34)–C(35)	1.369(6)
C(35)–C(36)	1.381(6)		
C(3)–N(1)–C(2)	111.6(3)	C(3)–N(1)–Li	117.8(3)
C(2)–N(1)–Li	123.6(3)	C(3)–N(2)–C(1)	117.2(3)
C(2)–N(3)–C(1)	118.2(3)	O(5)–Li–O(6A)	93.0(6)
O(5)–Li–O(4A)	99.7(8)	O(6A)–Li–O(4A)	103.2(6)
O(5)–Li–O(4)	99.5(8)	O(6A)–Li–O(4)	104.4(7)
O(6A)–Li–O(5A)	102.3(7)	O(4A)–Li–O(5A)	92.4(6)
O(4)–Li–O(5A)	92.0(7)	O(5)–Li–N(1)	116.9(5)
O(6A)–Li–N(1)	123.6(7)	O(4A)–Li–N(1)	115.8(5)
O(4)–Li–N(1)	115.0(6)	O(5A)–Li–N(1)	114.3(5)
O(5)–Li–O(6)	99.2(6)	O(4A)–Li–O(6)	98.8(5)
O(4)–Li–O(6)	100.0(6)	O(5A)–Li–O(6)	108.2(6)
N(1)–Li–O(6)	122.4(5)	C(44)–O(4)–C(41)	106.8(6)
C(44)–O(4)–Li	108.4(7)	C(41)–O(4)–Li	144.8(8)
O(4)–C(41)–C(42)	105.3(6)	C(43)–C(42)–C(41)	106.5(6)
C(42)–C(43)–C(44)	107.6(5)	O(4)–C(44)–C(43)	107.4(5)
C(44A)–O(4A)–C(41A)	106.4(6)	C(44A)–O(4A)–Li	128.7(6)
C(41A)–O(4A)–Li	118.9(6)	O(4A)–C(41A)–C(42A)	105.5(5)
C(43A)–C(42A)–C(41A)	107.9(4)	C(42A)–C(43A)–C(44A)	108.0(4)
O(4A)–C(44A)–C(43A)	106.8(5)	C(54)–O(5)–C(51)	106.8(6)
C(54)–O(5)–Li	128.8(9)	C(51)–O(5)–Li	124.1(8)
O(5)–C(51)–C(52)	105.6(6)	C(53)–C(52)–C(51)	107.7(5)
C(52)–C(53)–C(54)	108.2(4)	O(5)–C(54)–C(53)	106.7(5)
C(54A)–O(5A)–C(51A)	106.1(5)	C(54A)–O(5A)–Li	129.9(7)
C(51A)–O(5A)–Li	123.4(8)	O(5A)–C(51A)–C(52A)	106.1(5)
C(53A)–C(52A)–C(51A)	107.4(5)	C(52A)–C(53A)–C(54A)	107.9(4)
O(5A)–C(54A)–C(53A)	107.1(6)	C(61)–O(6)–C(64)	107.9(5)
C(61)–O(6)–Li	132.6(7)	C(64)–O(6)–Li	119.5(6)
O(6)–C(61)–C(62)	107.3(5)	C(63)–C(62)–C(61)	106.9(6)
C(62)–C(63)–C(64)	106.6(5)	O(6)–C(64)–C(63)	106.3(5)
C(64A)–O(6A)–C(61A)	108.2(5)	C(64A)–O(6A)–Li	134.5(8)
C(61A)–O(6A)–Li	116.9(7)	O(6A)–C(61A)–C(62A)	105.7(6)

Table 2 (continued)

C(63A)–C(62A)–C(61A)	105.7(6)	C(62A)–C(63A)–C(64A)	105.5(6)
O(6A)–C(64A)–C(63A)	106.4(6)	N(3)–C(1)–N(2)	114.5(3)
N(3)–C(1)–2C(12)	108.5(3)	N(2)–C(1)–C(12)	108.2(3)
N(3)–C(1)–C(11)	108.2(3)	N(2)–C(1)–C(11)	106.4(3)
C(12)–C(1)–C(11)	111.1(3)	C(111)–C(11)–C(113)	108.7(5)
C(111)–C(11)–C(112)	109.3(4)	C(113)–C(11)–C(112)	107.5(5)
C(111)–C(11)–C(1)	111.4(4)	C(113)–C(11)–C(1)	108.4(4)
C(112)–C(11)–C(1)	111.5(4)	C(13)–C(12)–C(1)	116.2(3)
C(12)–C(13)–C(14)	113.4(5)	C(15)–C(14)–C(13)	118.1(7)
N(3)–C(2)–N(1)	127.6(3)	N(3)–C(2)–C(21)	116.0(3)
N(1)–C(2)–C(21)	116.4(3)	C(26)–C(21)–C(22)	118.2(4)
C(26)–C(21)–C(2)	121.4(3)	C(22)–C(21)–C(2)	120.4(4)
C(21)–C(22)–C(23)	121.3(4)	C(24)–C(23)–C(22)	119.8(4)
C(23)–C(24)–C(25)	120.2(4)	C(24)–C(25)–C(26)	119.7(4)
C(21)–C(26)–C(25)	120.8(4)	N(2)–C(3)–N(1)	128.4(3)
N(2)–C(3)–C(31)	115.0(3)	N(1)–C(3)–C(31)	116.5(3)
C(36)–C(31)–C(32)	118.3(3)	C(36)–C(31)–C(3)	120.5(3)
C(32)–C(31)–C(3)	121.2(3)	C(33)–C(32)–C(31)	120.8(4)
C(34)–C(33)–C(32)	120.0(4)	C(33)–C(34)–C(35)	119.6(4)
C(34)–C(35)–C(36)	120.4(4)	C(31)–C(36)–C(35)	120.9(4)

cally- and geometrically-similar environment [a similar comparison has been made for the silazane cubic cage species $(MeSi)_2(N^tBu)_4Li_2$ [15] and $(MeSi)_2(N^tBu)_4(MgMe)_2$ [16]]. Association, prevalent in other Li and Mg organic derivatives is not a factor here, and it is for this reason above all that the structures are so alike. Within the monomeric arrangement each metal centre is four coordinate: Li bonds to 1N and 3O atoms, and Mg to 1C, 1N and 2O atoms. Hence, the higher-valency requirement of the alkaline-earth metal is in a coordination sense, equalised by extra solvation (i.e. 3 THF ligands instead of 2) of the Group 1 metal, but the former metal is the intrinsically stronger Lewis acid. Predictably the metal coordination geometries are pseudotetrahedral (range of bond angles: at Li, 92.0–123.7°; at Mg, 92.2–129.3°). Disorder in the THF ligands in both crystal structures diminishes the accuracy of the metal–donor bond lengths, but it is still significant that their ranges overlap (i.e. Li–O, 1.958–2.091 Å; Mg–O, 2.047–2.070 Å). More instructive is a comparison of the metallo-triazine dimensions. There is an insignificant difference in the lengths of the metal–N(1) bonds [i.e. 2.059(8) Å for Li, 2.067(3) Å for Mg]; these represent the only interaction between the metal and the C_3N_3 ring. Lying 0.24 Å out of the LiC(2)C(3) plane and 0.13 Å out of the MgC(2)C(3) plane, this three-coordinate N atom is only very slightly pyramidal (sum of angles at N(1): 353° in **11**; 358° in **18**). The distortion from planarity is greater when the whole C_3N_3 ring is considered: Li lies 1.23 Å out of the mean ring plane (which has a RMS deviation of 0.063 Å), and the Mg deviation is 0.92 Å (RMS deviation for ring atoms, 0.075 Å). The N(1) atom also bridges a pair of C atoms in this ring. Again the bonds are shorter, but in one case not significantly so, in the Li structure [i.e. C(2)–N(1), 1.386(4) Å vs. 1.389(4) Å; C(3)–N(1), 1.371(4) Å vs. 1.396(4) Å]. There is also no significant difference in the endocyclic ring angles at N(1) [111.6(3)° and 111.1(3)° for the Li and Mg structures respectively]. The formal C=N (double) bonds [C(2)–N(3), C(3)–N(2)] within the triazine rings seem to be shorter in the Mg case [i.e. 1.281(4) Å and 1.278(4) Å respectively, vs. 1.287(5) Å and 1.291(4) Å], but as before the differences are negligible. On average C=N bond lengths are about 1.28 Å [17] so clearly there is very little delocalisation of electron density in the C_3N_3 ring. The longest ring bonds by far are, as expected; those involving the saturated C atom [C(1)]; their mean lengths (1.466 Å in the Li structure, 1.477 Å in the Mg structure), are essentially the same as that usually observed for single (sp^3) C–N bonds (1.47 Å) [17]. Each C_3N_3 ring is distinctly puckered at this sp^3C atom, which lies 0.219 Å and 0.261 Å out of the mean plane of the other five ring atoms (rms deviations, 0.029 Å and 0.032 Å) in **11** and **18** respectively. The remaining endocyclic (C_3N_3) ring angles appear to be essentially unaffected by the identity of the metal cation attached to N(1) [i.e. N(2)/N(3), 117.7° (mean), C(2)/C(3), 128.0° (mean), C(1), 114.5(3)° for Li^+, vs. 117.9°, 128.0° and 113.9(3)° respectively for Mg^{2+}]. Overall, therefore, the greater ionicity of Li than Mg has only a very modest bearing on the electronic structure of the triazine heterocycle. Exceptionally, in the structure of **18**, the Mg–C bond has a length [2.164(3) Å] commensurate with those in pseudotetrahedral $Me_2Mg.L$ monomeric complexes [e.g. 2.17 Å when L = TMEDA [18]; 2.19 Å when L = $(quinuclidine)_2$ [19]]. Full lists of bond lengths and bond angles are given in Tables 2 and 3 for **11** and **18** respectively, and atomic coordinates in Tables 4 and 5.

Table 3
Bond lengths (Å) and angles (°) for **18**

Mg–N(1)	2.067(3)	Mg–O(4)	2.047(3)
Mg–O(5)	2.05(2)	Mg–C(6)	2.164(3)
Mg–O(5A)	2.07(2)	N(1)–C(2)	1.389(4)
N(1)–C(3)	1.396(4)	N(2)–C(3)	1.278(4)
N(2)–C(1)	1.474(4)	N(3)–C(2)	1.281(4)
N(3)–C(1)	1.480(4)	C(1)–C(12)	1.47(3)
C(1)–C(11)	1.578(5)	C(1)–C(12A)	1.58(3)
C(11)–C(111)	1.515(6)	C(11)–C(113)	1.537(6)
C(11)–C(112)	1.542(6)	C(12)–C(13)	1.51(2)
C(13)–C(14)	1.54(2)	C(14)–C(15)	1.46(2)
C(12A)–C(13A)	1.51(2)	C(13A)–C(14A)	1.53(2)
C(14A)–C(15A)	1.47(2)	C(2)–C(21)	1.498(5)
C(21)–C(26)	1.380(5)	C(21)–C(22)	1.393(5)
C(22)–C(23)	1.382(6)	C(23)–C(24)	1.359(6)
C(24)–C(25)	1.372(6)	C(25)–C(26)	1.389(5)
C(3)–C(31)	1.501(4)	C(31)–C(32)	1.389(5)
C(31)–C(36)	1.392(5)	C(32)–C(33)	1.387(5)
C(33)–C(34)	1.369(6)	C(34)–C(35)	1.366(6)
C(35)–C(36)	1.381(5)	O(4)–C(41)	1.414(8)
O(4)–C(44A)	1.44(2)	O(4)–C(44)	1.445(8)
O(4)–C(41A)	1.47(2)	C(41)–C(42)	1.485(10)
C(42)–C(43)	1.441(12)	C(43)–C(44)	1.496(10)
C(41A)–C(42A)	1.48(2)	C(42A)–C(43A)	1.45(3)
C(43A)–C(44A)	1.47(2)	O(5)–C(51)	1.416(14)
O(5)–C(54)	1.451(14)	C(51)–C(52)	1.480(14)
C(52)–C(53)	1.48(2)	C(53)–C(54)	1.50(2)
O(5A)–C(51A)	1.42(2)	O(5A)–C(54A)	1.44(2)
C(51A)–C(52A)	1.48(2)	C(52A)–C(53A)	1.47(2)
C(53A)–C(54A)	1.55(2)		
O(4)–Mg–O(5)	94.7(7)	O(4)–Mg–N(1)	105.98(12)
O(5)–Mg–N(1)	108.2(7)	O(4)–Mg–C(6)	107.90(14)
O(5)–Mg–C(6)	105.4(6)	N(1)–Mg–C(6)	129.30(14)
O(4)–Mg–O(5A)	92.2(9)	N(1)–Mg–O(5A)	108.3(8)
O(5A)–Mg–C(6)	106.9(7)	C(2)–N(1)–C(3)	111.1(3)
C(2)–N(1)–Mg	124.5(2)	C(3)–N(1)–Mg	122.4(2)
C(3)–N(2)–C(1)	117.9(3)	C(2)–N(3)–C(1)	117.8(3)
C(12)–C(1)–N(2)	112(2)	C(12)–C(1)–N(3)	107.4(14)
N(2)–C(1)–N(3)	113.9(3)	C(12)–C(1)–C(11)	109.1(10)
N(2)–C(1)–C(11)	106.8(3)	N(3)–C(1)–C(11)	107.4(3)
N(2)–C(1)–C(12A)	106(2)	N(3)–C(1)–C(12A)	110(2)
C(11)–C(1)–C(12A)	112.7(12)	C(111)–C(11)–C(113)	108.8(4)
C(111)–C(11)–C(112)	108.1(4)	C(113)–C(11)–C(112)	109.1(4)
C(111)–C(11)–C(1)	108.9(3)	C(113)–C(11)–C(1)	111.0(3)
C(112)–C(11)–C(1)	110.9(3)	C(1)–C(12)–C(13)	114(2)
C(12)–C(13)–C(14)	111(2)	C(15)–C(14)–C(13)	118(2)
C(13A)–C(12A)–C(1)	117(2)	C(12A)–C(13A)–C(14A)	113(2)
C(15A)–C(14A)–C(13A)	118(2)	N(3)–C(2)–N(1)	128.0(3)
N(3)–C(2)–C(21)	117.2(3)	N(1)–C(2)–C(21)	114.8(3)
C(26)–C(21)–C(22)	118.1(3)	C(26)–C(21)–C(2)	122.0(3)
C(22)–C(21)–C(2)	119.9(3)	C(23)–C(22)–C(21)	120.3(4)
C(24)–C(23)–C(22)	120.9(4)	C(23)–C(24)–C(25)	119.8(4)
C(24)–C(25)–C(26)	120.0(4)	C(21)–C(26)–C(25)	120.9(4)
N(2)–C(3)–N(1)	128.0(3)	N(2)–C(3)–C(31)	116.6(3)
N(1)–C(3)–C(31)	115.3(3)	C(32)–C(31)–C(36)	118.4(3)
C(32)–C(31)–C(3)	122.1(3)	C(36)–C(31)–C(3)	119.5(3)
C(33)–C(32)–C(31)	120.4(4)	C(34)–C(33)–C(32)	120.1(4)
C(35)–C(34)–C(33)	120.3(4)	C(34)–C(35)–C(36)	120.3(4)
C(35)–C(36)–C(31)	120.6(4)	C(41)–O(4)–C(44)	108.2(5)
C(44A)–O(4)–C(41A)	104(2)	C(41)–O(4)–Mg	132.0(4)
C(44A)–O(4)–Mg	133.8(10)	C(44)–O(4)–Mg	119.7(4)
C(41A)–O(4)–Mg	118.6(10)	O(4)–C(41)–C(42)	107.6(6)
C(43)–C(42)–C(41)	104.1(8)	C(42)–C(43)–C(44)	104.0(7)
O(4)–C(44)–C(43)	104.4(5)	O(4)–C(41A)–C(42A)	105(2)
C(43A)–C(42A)–C(41A)	104(2)	C(42A)–C(43A)–C(44A)	105.6(13)

Table 3 (continued)

O(4)–C(44A)–C(43A)	109.3(12)	C(51)–O(5)–C(54)	107.2(9)
C(51)–O(5)–Mg	134.9(13)	C(54)–O(5)–Mg	116.3(12)
O(5)–C(51)–C(52)	107.6(9)	C(53)–C(52)–C(51)	103.1(10)
C(52)–C(53)–C(54)	100.7(12)	O(5)–C(54)–C(53)	104.2(10)
C(51A)–O(4A)–C(54A)	104.2(13)	C(51A)–O(5A)–Mg	127.7(14)
C(54A)–O(5A)–Mg	127(2)	O(5A)–C(51A)–C(52A)	107.3(10)
C(53A)–C(52A)–C(51A)	106.1(10)	C(52A)–C(53A)–C(54A)	101.0(13)
O(5A)–C(54A)–C(53A)	101.5(14)		

2.6. *Ab initio MO calculations on 1,2-dihydrotriazine versus 1,4-dihydrotriazine structural options*

Dihydrotriazine compounds can adopt either 1,2-dihydro or 1,4-dihydro ring arrangements. Lithio types prefer the latter arrangement as evidenced by the crystal structure of the tris (THF) solvate **11**. But, interestingly, as reported in the original communication of this work, replacing Li^+ by H^+ (accomplished experimentally by methanolysis), causes the 1,4-dihydro form to be converted into its 1,2-dihydro analogue. To attempt to rationalise these contrasting preferences and to quantify the relative stabilities of the structural options involved, we have carried out a series of ab initio MO geometry optimisations [20] (at the 6-31G level [21]) on model systems.

Calculations on simple lithio models which do not take into account the effects of solvation indicate that the 1,4-dihydro structure (**19**) is energetically preferred to the 1,2-dihydro alternative (**20**), in accordance with what is found experimentally. They differ by 4.1 kcal mol^{-1} in relative terms, having total energies of −286.5742 au and −286.5677 au, respectively. Fig. 3 shows both structures as well as important bond lengths therein. The absence of solvation, coupled with the fact that calculated bond lengths are generally shorter than those determined by X-ray diffraction accounts for the substantially shorter N–Li bond in **19** (1.810 Å) (that in the crystal structure is (2.059 Å)). Also, by having hydrogen atoms attached to the C-sites of the triazine ring instead of the actual organic substituents, the ring of model **19** is virtually planar, whereas that of the crystal structure is non-planar, as discussed in Section 2.5. For the same reason, model **19** is not a good one from which to judge steric effects. More realistically, two methyl groups were substituted for the two hydrogen atoms on the saturated C atoms of the C_3N_3 rings, giving the new models **21** and **22**. Given the relative proximities of these methyl substituents to the Li^+ cation, this change might have been expected to destabilise the 1,2-dihydro structure. Surprisingly, this not the case as the energy difference between the two isomers actually falls to 2.76 kcal mol^{-1}, though, as previously, the 1,4-dihydro form is the more stable (total energy, −357.7398 au, cf −357.7372 au for **22**). This finding suggests that electronic effects outweigh steric ones. To examine the effect of correlation energy on the relative energies of the two configurations, **19** and **20**, the optimisation calculations were repeated at the MP2 level [22]. This exercise did not alter the energetic preference of the two isomers (1,4-dihydro: −287.1841 au; 1,2-dihydro: −287.1793 au), with an energy difference of 2.98 kcal mol^{-1}. When the influence of solvation at Li is considered, the energy gap between the isomers is even smaller, as shown by calculations on models **23** and **24**, in which ammonia molecules mimic the THF molecules of the crystal structure. Again the 1,4-dihydro entity (**23**) is lower in energy (more stable), but only by 0.22 kcal mol^{-1} (total energy, −455.1696 au vs. −455.1692 au for **24**). With steric effects less important, this small difference in stability can be attributed to similar electronic structures, with each isomer having five ring atoms (except for the saturated C atom) in conjugation. Comparison with the unsolvated 1,4-dihydro model **19** reveals that the overall energy gain due to solvation in **23** is 62.0 kcal mol^{-1}, which represents 20.7 kcal mol^{-1} per donor molecule. The structure of model **23** and selected bond lengths are shown in Fig. 4. Note that the C_3N_3 framework is essentially planar while the Li^+ cation sits 0.26 Å out of this plane. In addition, the N–Li bond is distinctly longer than in the unsolvated species **19** (i.e. 1.983 Å vs. 1.810 Å).

Interestingly, results from calculations on lithium-free dihydrotriazines (i.e. where Li^+ has been replaced by H^+), conflict with what is found in practice. As

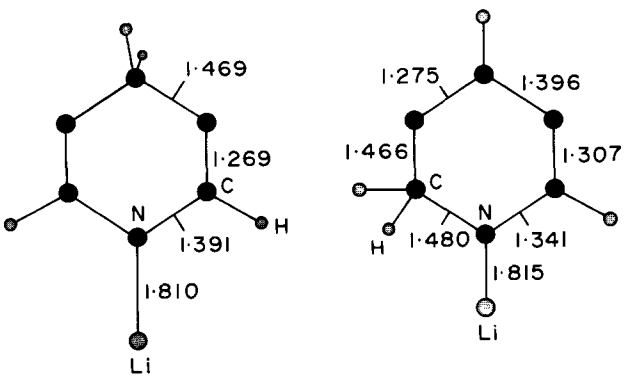

Fig. 3. Ab initio optimised geometries of the unsolvated lithiotriazine model compounds **19** and **20**, showing key bond lengths.

Table 4
Atomic coordinates ($\times 10^4$) for **11**

	x	y	z
N(1)	1054(2)	2067(2)	261(2)
N(2)	1513(2)	3177(2)	−459(2)
N(3)	2924(3)	1962(2)	−201(2)
Li	451(7)	2006(4)	1168(4)
O(4)	36(11)	3129(7)	1546(9)
C(41)	−950(11)	3653(10)	1691(11)
C(42)	−343(19)	4271(9)	2190(11)
C(43)	875(15)	4341(9)	2094(11)
C(44)	1151(12)	3602(11)	1710(12)
O(4A)	3(9)	3113(4)	1547(7)
C(41A)	−1241(9)	3235(6)	1667(8)
C(42A)	−1273(12)	4104(6)	1922(8)
C(43A)	−252(14)	4525(5)	1772(9)
C(44A)	484(12)	3926(5)	1455(8)
O(5)	1638(11)	1582(12)	1936(4)
C(51)	1288(10)	1210(11)	2519(5)
C(52)	2321(12)	1392(19)	3076(4)
C(53)	3348(10)	1588(16)	2801(6)
C(54)	2956(12)	1656(14)	2070(6)
O(5A)	1826(10)	1783(10)	1970(4)
C(51A)	1789(9)	2082(11)	2635(5)
C(52A)	3086(10)	2238(10)	2951(5)
C(53A)	3835(9)	1784(13)	2594(6)
C(54A)	3035(12)	1438(12)	1993(6)
O(6)	−1117(7)	1312(6)	1297(7)
C(61)	−1421(10)	449(7)	1215(11)
C(62)	−2652(12)	333(8)	1402(13)
C(63)	−3192(8)	1122(8)	1395(9)
C(64)	−2163(10)	1738(6)	1482(7)
O(6A)	−882(9)	1249(7)	1343(9)
C(61A)	−550(11)	629(8)	1857(7)
C(62A)	−1574(14)	9(7)	1756(10)
C(63A)	−2616(12)	442(11)	1422(11)
C(64A)	−2124(12)	1097(10)	1023(7)
C(1)	2758(3)	2817(2)	−462(2)
C(11)	2935(4)	2808(3)	−1211(2)
C(111)	28923(6)	3691(4)	−1514(3)
C(112)	4196(5)	2432(4)	−1284(3)
C(113)	1924(5)	2252(4)	−1611(3)
C(12)	3725(3)	3385(3)	−35(2)
C(13)	3685(4)	3419(3)	691(3)
C(14)	4663(6)	3994(4)	1080(4)
C(15)	4745(10)	4042(7)	1763(6)
C(2)	2123(3)	1674(2)	137(2)
C(21)	2365(3)	811(2)	416(2)
C(22)	3548(4)	469(3)	497(3)
C(23)	3791(4)	−331(3)	753(3)
C(24)	2848(5)	−800(3)	930(3)
C(25)	1654(4)	−486(3)	836(3)
C(26)	1418(4)	322(2)	585(2)
C(3)	806(3)	2787(2)	−112(2)
C(31)	−465(3)	3158(2)	−149(2)
C(32)	−1468(3)	2664(2)	−66(2)
C(33)	−2642(3)	3011(3)	−105(2)
C(34)	−2819(4)	3853(3)	−224(3)
C(35)	−1833(4)	4346(3)	−312(4)
C(36)	−665(4)	3998(3)	−281(3)

Table 5
Atomic coordinates ($\times 10^4$) for **18**

	x	y	z
Mg	7708.5(9)	220.7(8)	8284.8(7)
N(1)	7388(2)	−654(2)	7354(2)
N(2)	6187(2)	−985(2)	6189(2)
N(3)	8066(2)	−1374(2)	6195(2)
C(1)	7069(3)	−1231(2)	5604(2)
C(11)	6749(3)	−2090(3)	5256(2)
C(111)	6590(4)	−2746(3)	5917(3)
C(112)	5711(4)	−1998(3)	4719(3)
C(113)	7612(4)	−2396(3)	4704(3)
C(12)	7276(30)	−601(15)	5054(19)
C(13)	7514(35)	270(15)	5395(16)
C(14)	7987(26)	832(13)	4734(17)
C(15)	8494(27)	1612(14)	5015(16)
C(12A)	7198(33)	−491(17)	5052(21)
C(13A)	7754(33)	294(16)	5376(18)
C(14A)	7678(30)	1027(14)	4759(18)
C(15A)	8023(36)	1860(15)	5059(21)
C(2)	8148(3)	−1074(2)	6933(2)
C(21)	9169(3)	−1206(2)	7426(2)
C(22)	10108(3)	−1194(3)	7029(2)
C(23)	11056(3)	−1306(3)	7480(3)
C(24)	11091(3)	−1449(3)	8312(3)
C(25)	10175(4)	−1486(3)	8713(3)
C(26)	9216(3)	−1364(2)	8270(2)
C(3)	6402(3)	−719(2)	6929(2)
C(31)	5487(3)	−486(2)	7423(2)
C(32)	5482(3)	−642(2)	8270(2)
C(33)	4613(3)	−432(3)	8703(3)
C(34)	3752(3)	−70(3)	8296(3)
C(35)	3741(3)	83(3)	7461(3)
C(36)	4598(3)	−128(3)	7021(2)
O(4)	6813(2)	1254(2)	7965(2)
C(41)	6564(16)	1650(8)	7192(5)
C(42)	5926(12)	2408(8)	7353(6)
C(43)	6182(7)	2594(4)	8217(5)
C(44)	6369(9)	1749(6)	8607(5)
C(41A)	6667(55)	1485(30)	7085(14)
C(42A)	6220(41)	2346(23)	7087(19)
C(43A)	5549(28)	2342(21)	7782(24)
C(44A)	5975(25)	1686(21)	8347(16)
O(5)	9108(11)	790(16)	8075(13)
C(51)	9636(15)	1005(20)	7359(12)
C(52)	10744(13)	1185(18)	7628(11)
C(53)	10684(13)	1442(13)	8506(10)
C(54)	9871(14)	839(13)	8781(10)
O(5A)	9084(14)	839(21)	8043(16)
C(51A)	9375(15)	1165(21)	7272(13)
C(52A)	10522(14)	1306(20)	7347(12)
C(53A)	10868(12)	1093(17)	8208(14)
C(54A)	9832(17)	1200(16)	8645(12)
C(6)	7715(3)	67(2)	9619(2)

stated earlier, methanolysis of a lithio 1,4-dihydro species affords a 1,2-dihydrotriazine, but the ab initio model thereof (**25**) is predicted to be 2.36 kcal mol^{-1} less stable than the model 1,4-dihydrotriazine (**26**) (total energies: −279.6869 au and −279.6907 au respectively). This contradiction prompted a theoretical appraisal of the lithiotriazine/methanol reaction. In the experimental case, methanol was added to the tris (THF) solvated lithio 1,4-dihydro species. This process was simulated theoretically by adding methanol to the tris (NH_3) solvated model. When it was placed near to

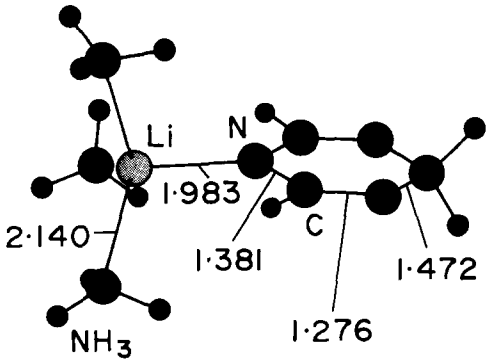

Fig. 4. Ab initio optimised structure of the tris(ammonia) solvate **23**, showing key bond lengths.

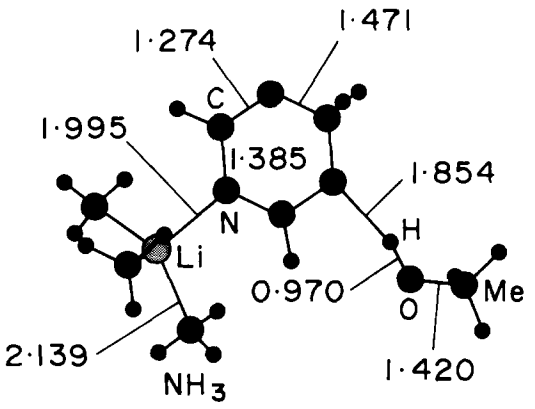

Fig. 5. Ab initio optimised geometry of the lithiotriazine methanolate intermediate **27**, showing key bond lengths.

the solvated Li^+ centre, no O–Li bond was formed; instead methanol preferred to move away (the calculation was abandoned when the O...Li separation distance exceeded 3.7 Å). Thus solvation of the Li^+ centre effectively blocks the formation of MeOLi and the 1,4-dihydrotriazine via this route. In contrast, however, a stable complex (**27**) resulted when methanol approached the C_3N_3 ring at the N atom located at the "2" position (i.e. adjacent to the saturated C atom). Its total energy −570.1784 au, which represents a stabilisation of 11.5 kcal mol^{-1} over free methanol and the triazine species in question. Fig. 5 shows this structure and gives selected bond lengths. As can be seen, methanol binds to the heterocyclic ring via its H atom. The new N–H bond measures 1.854 Å in length. This complexation causes an elongation of the N–Li bond from 1.983 Å in model **23** to 1.995 Å. The implication here is that the N–Li bond is on the way to breaking, to release Li^+, while, concomitantly, the N–H bond is shortening further, causing the OH bond to lengthen and ultimately to cleave, to give MeO^-. In complete agreement with experimental findings, the final products associated with this process would be MeOLi and the 1,2-dihydrotriazine.

Thus, in conclusion, ab initio MO geometry optimisations confirm that lithiotriazines prefer 1,4-dihydro arrangements to 1,2-dihydro alternatives for thermodynamic reasons, but that the products of subsequent methanolysis adopt the latter isomeric form as a result of mechanistic considerations.

3. Experimental

3.1. Syntheses

The same general procedure was followed in synthesising, and where applicable crystallising, triazine and

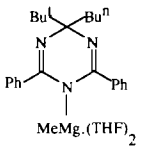

18

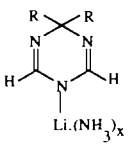

19 ; R=H , x=0

21 ; R=Me , x=0

23 ; R=H , x=3

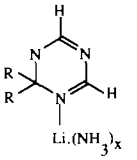

20 ; R=H , x=0

22 ; R=Me , x=0

24 ; R=H , x=3

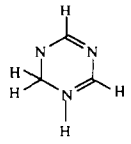

25

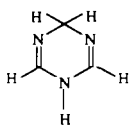

26

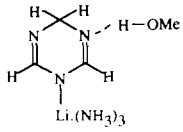

27

dihydrotriazine products, and so only the syntheses of **1**, **11** and **18**, which serve as typical examples, are presented in full.

1. Benzonitrile (30 mmol) was added dropwise (from a syringe) to a chilled solution of *n*-butyllithium (10 mmol) in hexane contained in a Schlenk tube under dry oxygen-free argon. An insoluble polymeric orange gum was formed almost instantly, sticking to the side of the glass tube. Subsequent addition of THF (ca 5 ml) dissolved the gum, to give a dark red solution. Cooling to 0°C afforded a crop of colourless needles. After removal of this solid by filtration, cooling the filtrate to −20°C gave a further batch of solid. Both batches were identified as the simple (metal-free) triazine **1**.

11. Slow addition of trimethylacetonitrile (10 mmol) to a chilled hexane solution of *n*-butyllithium (10 mmol) generated the pale green solution of the imidolithium ^{t}Bu(^{n}Bu)C=NLi. Subsequent dropwise addition of benzonitrile (20 mmol) resulted in separation of an orange oil, which was dissolved by mild heating and addition of THF (5 ml) to give an orange solution. Rapid cooling to −20°C precipitated a yellow solid, which was redissolved by raising the temperature. Subsequent slow cooling during 24 h produced a large crop of yellow crystals identified as the air- and moisture-sensitive lithio dihydrotriazine tris (THF) solvate **11**.

18. Toluene (8 ml) was added to 5 mmol of freshly prepared crystalline **11** contained in a Schlenk tube filled with argon. The mixture was heated until the crystals dissolved. Methylmagnesium chloride (5 mmol) in THF was subsequently dripped into this yellow solution, producing a white precipitate (LiCl), which was removed by filtration. Cooling the filtrate overnight produced a microcrystalline solid. This was redissolved by warming the mixture. Crystals of a quality suitable for X-ray diffraction study were then grown by keeping the solution in a water bath maintained at 36°C for 24 h. Identified as the magnesio species **18**, these crystals were, like **11**, found to be air- and moisture-sensitive, as were all the metallo products obtained from the other reactions.

Table 6 records yields and physical/microanalytical data for the metallodihydrotriazine products discussed in Section 2. Analyses (C, H and N) were carried out with a Perkin-Elmer 240 elemental analyser of (Li and Mg) with a Philips PU 9100X flame atomic absorption spectrometer.

3.2. ^{1}H NMR spectra (400 MHz, 298 K)

2: ^{n}Bu (CH_3, 3H, t, δ0.82; γCH_2, 2H, m, δ1.27; βCH_2, 2H, quin, δ1.39; αCH_2, 2H, t, δ1.88) THF (βCH_2, 12H, t, δ1.76; αCH_2, 12H, t, δ3.62) Ph (*pH*, 1H, t, δ6.95; *m*H, 2H, t, δ7.09; *o*H, 2H, d, δ7.84) Ph′(*mH*, *p*H, 6H, m, δ7.28; *oH*, 4H, d, δ8.27). **7**: ^{n}Bu(CH_3, 3H, t, δ0.82; γCH_2, 2H, m, δ1.26; βCH_2, 2H, quin, δ1.43; αCH_2, 2H, t, δ1.93) THF (βCH_2, 8H, t, δ1.78; αCH_2, 8H, t, δ3.62). Ph(*p*H, 1H, t, δ6.99; *m*H, 2H, t, δ7.12; *o*H, 2H, d, δ7.80) Ph′(*m*H, *p*H, 6H, m, δ7.33; *o*H, 4H, d, δ8.27) PhC≡N (*m*H, 2H, t, δ7.50; *pH*, 1H, t, δ7.60; *oH*, 2H, d, δ7.68). **8**: ^{t}Bu(9H, s, δ1.03) THF (βCH_2, 8H, t, δ1.76; αCH_2, 8H, t, δ3.62) Ph (*p*H, 1H, t, δ6.96; *m*, 2H, t, δ7.05; *o*, 2H, d, δ7.88) Ph′ (*m*H, *p*H, 6H, m, δ7.28; *o*H, 4H, d, δ8.30) PhC≡N (*m*H, 2H, t, δ7.50; *p*H, 1H, t, δ7.60; *o*H, 2H, d, δ7.69). **10**: ^{t}Bu (9H, s, δ1.01) THF (βCH_2, 12H, t, δ1.76; αCH_2, 12H, t, δ3.62) Ph (*pH*, 1H, t, δ6.95; *m*H, 2H, t, δ7.05; *oH*, 2H, d, δ7.85) Ph′ (*m*H, *pH*, 6H, m, δ7.28; *o*H, 4H, d, δ8.27). **11**: ^{n}Bu (CH_3, 3H, t, δ0.81; βCH_2, 2H, quin, δ1.23; γCH_2, 2H, m, δ1.32; αCH_2, 2H, t, δ1.61) ^{t}Bu (9H, s, δ1.02) THF (βCH_2, 12H, t, δ1.76; αCH_2, 12H, t, 3.62) Ph (*m*H, *p*H, 6H, m, δ7.23; *o*H, 4H, d, δ8.05). **18** Me (3H, s, δ − 0.94) ^{n}Bu(CH_3, 3H, t, δ0.85; βCH_2, 2H, m, δ1.39; γCH_2, 2H, m, δ1.60; αCH_2, 2H, t, δ2.09) THF (βCH_2, 8H, m, δ0.95; αCH_2, 8H, m, δ3.02) Ph (*p*H, 1H, m, δ7.09; *mH*, 4H, t, δ7.23; *o*H, 4H, d, δ8.28). Spectra were recorded on a Bruker AMX400 spectrometer. Chemical shifts are quoted relative to $SiMe_4$ at δ0.00 ppm. The solvent employed was tetrahydrofuran-d_8 (except for **18**; toluene-d_8), and solutions were prepared in a glove box and tubes subsequently sealed under argon gas. Assignments were verified by "Cosy 45" experiments.

3.3. X-ray crystallographic studies

Crystal data for **11**: $C_{35}H_{52}LiN_3O_3$, $M = 569.7$, monoclinic, space group $P2_1/n$, $a = 10.917(2)$, $b =$

Table 6
Physical and microanalytical data for metallodihydrotriazine solid products

Product	Colour	Yield (%)	Melting point (°C)	Molecular formulae	Microanalysis (%) [a]			
					C	H	M	N
2	Pale yellow	79	102–104	$C_{37}H_{48}LiN_3O_3$	72.1(75.4)	9.0(8.1)	1.2(1.2)	7.1(7.1)
7	Yellow	39	77– 78	$C_{40}H_{45}LiN_4O_2$	74.3(79.2)	7.5(7.5)	1.1(1.2)	7.3(6.9)
8	Pale pink	54	90– 92	$C_{40}H_{45}LiN_4O_2$	78.4(79.2)	7.8(7.5)	1.1(1.2)	7.3(6.9)
10	Pale yellow	91	110–112	$C_{37}H_{48}LiN_3O_3$	73.0(75.4)	8.6(8.1)	1.3(1.2)	7.6(7.1)
11	Yellow	88	82– 84	$C_{35}H_{62}LiN_3O_3$	71.4(73.8)	9.6(9.1)	1.2(1.2)	7.0(7.4)
18	Colourless	57	168–170	$C_{32}H_{57}MgN_3O_2$	72.1(71.3)	9.3(9.4)	4.4(4.8)	8.3(8.3)

[a] Calculated values in parentheses.

15.893(3), c = 20.227(4) Å, β = 100.30(2)°, V = 3452.9(11) Å^3, $Z = 4$, $D_c = 1.096$ g cm^{-3}, $\mu = 0.54$ mm^{-1} for CuKα radiation ($\lambda = 1.54184$ Å), $F(000) = 1240$. Unit cell parameters were refined from 2θ values (30–40°) of 32 reflections measured at $\pm\omega$ on a Stoe-Siemens diffractometer. Intensities were measured with ω/θ scans and an on-line profile fitting procedure [23], from a crystal of size 0.71 × 0.62 × 0.54 mm. No significant variation was observed in the intensities of five standard reflections monitored at regular intervals.

The structure was determined by direct methods [24] and refined on F^2 by full-matrix least squares methods [25] from 5736 independent reflections ($2\theta_{max}$ = 130°), with a weighting scheme $W^{-1} = \sigma^2(F_0^2) + (aP)^2 + (bP)$, where $P = (F_0 + 2F_c)/3$, $a = 0.16$, b = 2.68. Hydrogen atoms were constrained to lie in geometrically predicted positions with isotopic displacement parameters tied to the equivalent values for their bonded atoms. All other atoms were assigned anisotropic parameters. Two-fold disorder was resolved for all three THF ligands and was refined with the aid of restraints on geometry and on atomic displacement parameters; the site occupation factors for the major disorder components of the three ligands refined to 57.2(12), 52.8(10) and 53.6(9)%. All shift/esd ratios were < 0.1 in the final refinement cycle.

For all reflections, $R^1 = [\Sigma w(F_0^2 - F_c^2)^2 / \Sigma w(F_0^2)^2]^{1/2} = 0.336$; the conventional $R = 0.092$ for F values of 3508 reflections with $F_0^2 > 2\sigma(F_0^2)$; goodness of fit = 0.996 on F^2 values for all data, 522 parameters and 384 restraints. All features in a final difference synthesis lie between +0.50 and −0.28e Å^{-3}.

Crystal data for **18**: $C_{32}H_{47}MgN_3O_2$, M = 530.0, monoclinic, space group $P2_1/c$, a = 12.756(3), b = 15.899(2), c = 16.118(3) Å, β = 93.667(4)°, V = 3262.2(11) Å^3, $Z = 4$, $D_c = 1.079$ g cm^{-3}, $\mu = 0.084$ mm^{-1} for Mo Kα radiation ($\lambda = 0.71073$ Å), $F(000)$ = 1152. Measurements were made as for **11** (2θ = 20–25°) for cell refinement, crystal size 0.69 × 0.38 × 0.37 mm).

The structure was determined and refined as above from 5732 independent reflections ($2\theta_{max} = 50°$), with weighting parameters $a = 0.0807$, $b = 1.9659$. Disorder was resolved for the THF ligands [major components 79.0(13)% and 52(2)%] and also for the n-butyl chain [53(4)%].

All shift/esd ratios were < 0.03. $R^1 = 0.210$ for all reflections, conventional $R = 0.057$ for F values of 2875 reflections with $F_0^2 > 2\sigma(F_0^2)$; goodness of fit = 1.057 on F^2 values for all data, 469 parameters and 183 restraints. All features in a final difference synthesis lie between +0.31 and −0.22e Å^{-3}.

For both compounds tables of anisotropic thermal parameters and hydrogen atom coordinates have been deposited at the Cambridge Crystallographic Data Centre.

Acknowledgments

We thank the SERC for providing financial support.

References

[1] A. Albert, *Heterocyclic Chemistry*, Athlone, London, 2nd edn., 1968; R.M. Acheson, *An Introduction to the Chemistry of Heterocyclic Compounds*, Wiley, New York, 2nd edn., 1967; E.M.R. Smolin and L. Rapoport, *The Chemistry of Heterocyclic Compounds*, Vol. 13, Wiley, New York, 1959; T.L. Gilchrist, *Heterocyclic Chemistry*, Longman, Harlow, 2nd edn., 1992.
[2] B.J. Wakefield, *The Chemistry of Organolithium Compounds*, Pergamon, Oxford, 1974; B.J. Wakefield, *Organolithium Methods*, Academic Press, London, 1988.
[3] R.M. Anker and A.H. Cook, *J. Chem. Soc.*, (1941) 323.
[4] A.L. Weis, Recent advances in the chemistry of dihydroazines, in A.R. Katritzky (ed.), *Advances in Heterocyclic Chemistry*, Academic Press London, 1985, pp. 91–103.
[5] D.R. Armstrong, W. Clegg, M. MacGregor, R.E. Mulvey and P.A. O'Neil, *J. Chem. Soc., Chem. Commun.*, (1993) 608.
[6] D.R. Armstrong, D. Barr, R. Snaith, W. Clegg, R.E. Mulvey, K. Wade and D. Reed, *J. Chem. Soc., Dalton Trans.*, (1987) 1071; D. Barr, R. Snaith, W. Clegg, R.E. Mulvey and K. Wade, *J. Chem. Soc., Dalton Trans.*, (1987) 2141.
[7] L.S. Cook and B.J. Wakefield, *J. Chem. Soc., Perkin Trans. 1*, (1980) 2392.
[8] T. Kottke and D. Stalke, *Angew. Chem., Int. Ed. Engl., 32* (1993) 580; *Angew. Chem., 105* (1993) 619.
[9] L.S. Cook, G. Prudhoe, N.D. Venayak and B.J. Wakefield, *J. Chem. Research* (M), (1982) 1357.
[10] K. Gregory, P.v.R. Schleyer and R. Snaith, *Adv. Inorg. Chem., 37* (1991) 47; R.E. Mulvey, *Chem. Soc. Rev., 20* (1991) 167.
[11] P.C. Andrews, D.R. Armstrong, M. MacGregor, R.E. Mulvey and D. Reed, *J. Chem. Soc., Chem. Commun.*, (1989) 1341.
[12] A.R. Sanger, *Inorg. Nucl. Chem. Lett., 9* (1973) 351.
[13] W.N. Setzer and P.v.R. Schleyer, *Adv. Organomet. Chem., 24* (1985) 353.
[14] P.R. Markies, O.S. Akkerman, F. Bickelhaupt, W.J.J. Smeets and A.L. Spek, *Adv. Organomet. Chem., 32* (1991) 147.
[15] M. Veith, F. Goffing and V. Huch, *Chem. Ber., 121* (1988) 943.
[16] M. Veith, F. Goffing and V. Huch, *Z. Naturforsch, B43* (1988) 846.
[17] F.H. Allen, O. Kennard, D.G. Watson, L. Brammer, A.G. Orpen and R. Taylor, *J. Chem. Soc., Perkin Trans, 2* (1987) 51.
[18] T. Greiser, J. Kopf, D. Thoennes and E. Weiss, *J. Organomet. Chem., 191* (1980) 1.
[19] J. Toney and G.D. Stucky, *J. Organomet. Chem., 22* (1970) 241.
[20] M. Dupuis, D. Spangler, J. Wendolowski, *NRCC Software Catalog*, Vol. 1, Program No. QG01 GAMESS; M.F. Guest, P. Fantucci, R.J. Harrison, J. Kendrick, J.H. van Lenthe, K. Schoeffel, P. Sherwood, GAMESS-UK (CFS Ltd, 1993).
[21] W.J. Hehre, R. Ditchfield and J.A. Pople, *J. Chem. Phys., 56* (1972) 2257; P.C. Hariharan and J.A. Pople, *Theor. Chim. Acta, 28* (1973) 213.
[22] C. Moller and M.S. Plesset, *Phys. Rev., 46* (1934) 618.
[23] W. Clegg, *Acta Crystallogr., Sect. A, 37* (1981) 22.
[24] H. Wang and B.E. Robertson, in A.J.C. Wilson (ed.), *Structure and Statistics in Crystallography*, Adenine, New York, 1985, p. 125.
[25] G.M. Sheldrick, SHELXL92, *Program for Crystal Structure Refinement*, University of Göttingen, 1992.